Proceedings of PSFVIP-5
5th Pacific Symposium on Flow Visualisation and Image Processing
27-29th September, 2005, Australia

PSFVIP-5-262

FLOW VISUALIZATION OF MICRO SYNTHETIC JETS

V. Timchenko*, J. Reizes and E. Leonardi

School of Mechanical and Manufacturing Engineering
The University of New South Wales, Sydney 2052, Australia.

*Corresponding author: Fax +61 2 9663 1222 Email: victoria@cfd.mech.unsw.edu.au

Abstract: The evolution of micro synthetic jet in a still ambient has been studied numerically. Unsteady computations of incompressible laminar flow have been performed for an axisymmetric numerical formulation for an orifice diameter of 50 μm. The diaphragm was assumed to oscillate sinusoidally in time and parabolically in space. Vortex pair trajectories were visualized by extracting the vortex cores from the flow data. It was demonstrated that centreline jet velocity reveals the propagation of vortex rings and dynamics of its peak value corresponds to the movement of the vortex cores. Furthermore, it was shown that the location of maximum vorticity could not be used to identify the location of the core.

1 Introduction

Synthetic jets [1] are jets which are produced by an oscillatory flow without net mass addition and therefore can be formed from the working fluid. A micro synthetic jet can be developed by a MEMS based actuator [2], which consists of an oscillating membrane in a cavity with an orifice in the face opposite the membrane. As the membrane oscillates, fluid is periodically expelled from and entrained into the cavity through the orifice. When a circular orifice is used a vortex ring can be formed at the edge of the orifice during the expulsion part of the cycle. Under appropriate conditions the vortex ring is not re-ingested into the orifice during the suction part of the cycle and as a result, a fluctuating, but continuous flow is generated away from the orifice.

Glezer and Amitay [1] described the formation of synthetic jets when successive vortex rings which have been shed from the orifice travel downstream, away from the orifice, forming a so-called vortex train. They studied synthetic jet in the Reynolds number range, $104 \le Re \le 489$, with $Re = \bar{V}d / \nu$, in which $\bar{V}$ is the average orifice expulsion velocity, d is the orifice diameter, and ν is the kinematic viscosity. This Reynolds number range is well outside likely applications to micro-jets which have extended potential applications e.g. [3]. Since the previously accepted criterion [4] that the inverse of the Strouhal number, defined as $St = \omega d / \bar{V}$, in which $\omega = 2\pi f$ and f is the frequency of oscillation of the diaphragm, should be greater than a constant value of 0.16 for axisymmetric synthetic jet formation had been developed on macro-sized jets, there was a need to establish whether this criterion could be applied to micro jets. Thus, in our earlier paper [5] we studied micro jets in the range $6.5 \le Re \le 35$. We found that the vortex ring, created near the orifice, travels only a short distance and is then amalgamated into a nearly stationary toroidal vortex, hereby called a lingering vortex, generated in previous cycles in the manner similar to the turbulent synthetic jet described by Mallinson *et al*. [6].

We also found that the above mentioned criterion [4] was in fact inadequate so that we studied conditions for the formation of micro synthetic jets and developed a criterion, which determines the onset of the sustained jet regime [5]. The newly developed criterion is unfortunately more complex than the earlier criterion being a function of the jet Reynolds number, *Re*, and either the Stokes number, $S = \sqrt{\omega d^2/\nu}$, or the Strouhal number, since the two are related, viz, $St = \omega d/\bar{V} = S^2/Re$. In order to establish a criterion, results were obtained for axisymmetric micro synthetic jets for $250 \le f \le 50{,}000$ *Hz*, with orifice diameters $20 \le d \le 200$ μm which leads to a Stokes number range, $0.2 \le S \le 7.2$. We defined a jet to exist if at all times there is a positive velocity, that is velocity directed away from the orifice, anywhere along the jet centre-line. Of course, this needed to be quantified. We stipulated that if V_{min}, the smallest maximum velocity during a cycle is always positive and if its value is in the range: $0.05\% < (V_{\min}/\bar{V}) < 0.1\%$, then this is an incipient jet and the conditions for this jet to be formed were used to establish the criterion. The upper and lower bounds for determining the incipient jet were chosen because they were sufficiently large to indicate that positive velocity really exists but sufficiently small to indicate a first occurrence.

In this work we concentrate on the study of the evolution of micro synthetic jets in a still ambient using flow visualization so as to determine the motion of the vortices and attempt to evaluate their interaction with the jet.

2. Simulation Methodology

In this study flows with Knudsen number, $Kn = \lambda/d < 0.01$ (λ is a mean free path of molecules), are modelled, so that the continuum approach using conventional conservation equations is valid [7]. Timchenko *et al*. [8] have demonstrated that the assumption of incompressible flow is valid for orifice diameters larger than 40 μm, whether the fluid is compressible or not. Therefore, a diameter of 50 μm is adopted in this study so that an incompressible approach is adequate. The set of unsteady conservation equations for laminar incompressible flow with constant properties consists of the continuity equation

$$\nabla \cdot \tilde{U} = 0 \tag{1}$$

and the Navier-Stokes equation,

$$\rho \frac{\partial \tilde{U}}{\partial t} + \rho \nabla \cdot (\tilde{U}\tilde{U}) = -\nabla p + \mu \nabla^2 \tilde{U} + \rho \tilde{g}\ , \tag{2}$$

in which, ρ, $\tilde{U}$, p, μ, t and $\tilde{g}$ denote the density, the velocity vector, the thermodynamic pressure, the dynamic viscosity, the time and the gravitational acceleration vector respectively.

The flow generated by synthetic jet actuators has been simulated using the commercial finite-volume package, CFX-5.6. Unsteady computations of the flow produced by synthetic jet actuator have been performed for the axisymmetric configuration shown in Figure 1.

The diameter of the diaphragm, W, was 1 mm, and the cavity depth, H was 550 μm. The length of the orifice h was 100 μm. The external cylindrical domain was 2.5mm in diameter (= 50d) and 2mm high (= 40d). In order to reduce the computational time the displacement of the membrane was simulated by replacing the diaphragm motion by its upward velocity at any point and any time, namely,

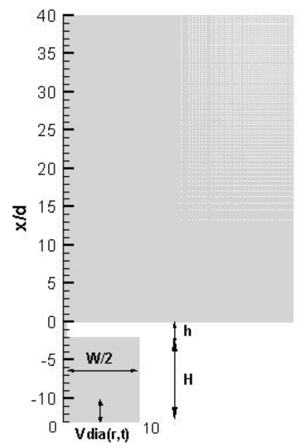

Figure 1. Computational domain

$$V_{dia}(r,t) = A\omega\left(1-\left(\frac{r}{(W/2)}\right)^2\right)\cos(\omega t)\,, \qquad (3)$$

which represents an inlet velocity at the diaphragm boundary. Here V_{dia} is the velocity in the direction normal to the diaphragm, hereby called the x direction and r is the radial variable.

We have shown that the use of equation (3) instead of the actual diaphragm motion leads to the same results at the same frequency and amplitude A, but significantly reduces the CPU time needed to obtain a solution. This is because a fixed mesh is employed rather then modelling the deflecting diaphragm with a deformable mesh. The pressure expressed as a gauge pressure was set to zero at the boundaries of the external domain.

The non-dimensional time, t, is defined as the ratio of the physical time to the period of oscillation, T, and the non-dimensional velocity is obtained by dividing the actual velocity by the average expulsion velocity, $\bar{V}$ at the exit from the orifice given by:

$$\bar{V} = \frac{2}{T}\frac{4}{\pi d^2}\int_0^{d/2}\int_0^{T/2} V_o(r,t)2\pi r dt dr\,, \qquad (4)$$

A second order backward Euler differencing scheme was used for the transient term, whereas a second order upwind differencing scheme was used for the advection terms. A time step of $T/200$ was used in all the results presented ($T = 2\pi/\omega$, is the period of the diaphragm oscillation in Equation 3). At each time step, the internal iterations were continued until the normalised mass and momentum residuals had been reduced to at least 10^{-6}. The numbers of grid points used for the cavity, the orifice and the external domain were 110 x 101, 50 x 16 and 358 x 200 in the x and r directions respectively, a total of 226,136 grid points. These values were chosen after a careful grid sensitivity study.

The validation of the axisymmetric configuration for synthetic jet actuator has already been performed [5] and will not be repeated here.

3. Results and Discussion

Two typical scenarios identified in [5] are considered here. One is with Re=7.5 when a jet has just been formed and satisfies the condition defining a jet to exist, whilst the other is at Re=23.5 when a jet has been well formed. These two cases cover the likely range of effects to be found with micro jets. The diaphragm is assumed to move parabolically in space and sinusoidally in time with a frequency of 1500 *Hz*. The orifice diameter was 50 μm and a fluid modelled was air at atmospheric pressure and 20^0C leading to a Stokes number of 1.25.

The trajectories of the toroidal vortices were visualized by extracting the vortex cores manually from the flow data. Previous authors, e.g. [9] had used the position of the maximum vorticity as an indication of the location of the vortex core, unfortunately, as will be shown later this is not correct. Similarly the two methods available in CFD Analyzer, an add-on to Tecplot 10.10, were unable to locate the cell centres consistently. CFD Analyzer did not yield realistic results, and this is despite the fact that the vorticity vector method, one of the methods recommended by Roth [10], was used to attempt to locate the cores.

A comparison of cycle-to-cycle results was used to establish that flow fields were approximately periodic after $3T$, from the start of the calculations. All the results presented in this paper were therefore obtained during the fourth cycle.

Velocity fields at different instants of the fourth cycle for Re=7.5 are presented in Figure 2. Due to the large difference between the magnitudes of the velocity vectors we show the velocity field in two ways; in the right hand side figures the lengths of the velocity vectors are proportional to the magnitude of the velocity and the area visualised has been restricted to region near the orifice, whereas, on the left hand side velocity vectors are of equal length but coloured by the magnitude of the non-dimensional axial velocity. This has been done to clerify that part of the field obscured by the long vectors on the right hand side of Figure 2 and to visualise the whole flow field as a whole.

The flow field shown in Figure 2a occurs at t=4.0, when the diaphragm is moving with maximum positive velocity, that is at the instant of maximum expulsion. It can be seen in Figures 2a and 2b that a newly emerging vortex is being generated at the edge of the orifice by the expelled fluid. This jet entrains some of the external fluid thereby causing the vortex to form. Note that towards the end of the expulsion stage (Figure 2b) the vortex is still attached. During the ingestion period, at t=4.4 (Figure 2c) the vortex has detached and is moving away from the orifice. It should be noted that the centreline velocity remains positive only in a restricted area (Figures 2c-2d) and that the remainder of the flow field is directed towards the orifice.

The use of $0.05\% < (V_{\min} / \bar{V}) < 0.1\%$ as the criterion for determining whether the jet exists has led to the identification of a small island of positive velocity in a sea of fluid moving in the opposite direction, as a “jet”. Whether this can be accepted as a jet or not is not at this stage clear.

The distribution of the axial velocity along the centreline for the suction stage is shown in Figure 3. This is totally unlike what happens when steady jet issues from a nozzle. Its centreline velocity has maximum value at the nozzle. Downstream, the centreline velocity remains constant in the potential core and then gradually reduces further out. As may be seen in Figure 3, during the injestion part of the cycle, ($4.25 < t < 4.75$) the velocity on the centre line of the “jet” is negative at the nozzle exit, gradually increasing downstream until a positive maximum is reached. Futher downstream the velocity decreases and, in fact, becomes slightly negative! This is in agreement with Figures 2(a) and 2(b), but entirely different to a steady jet!

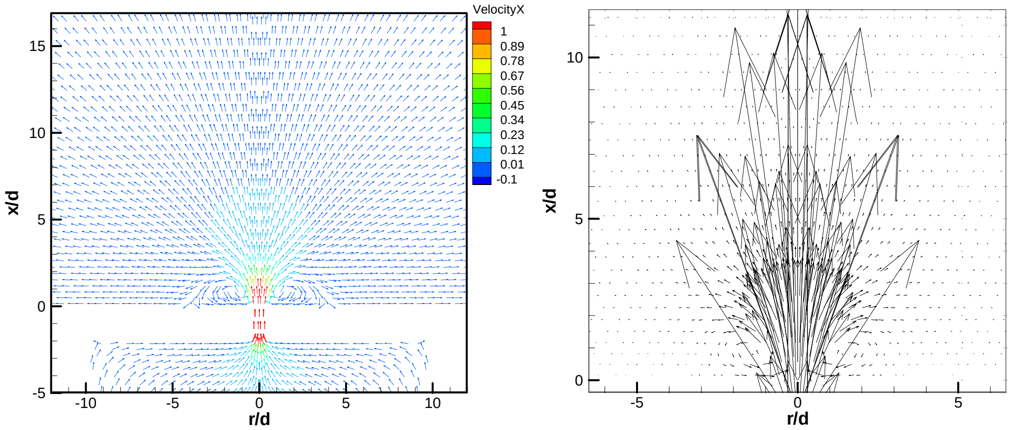

(a) t=4.0

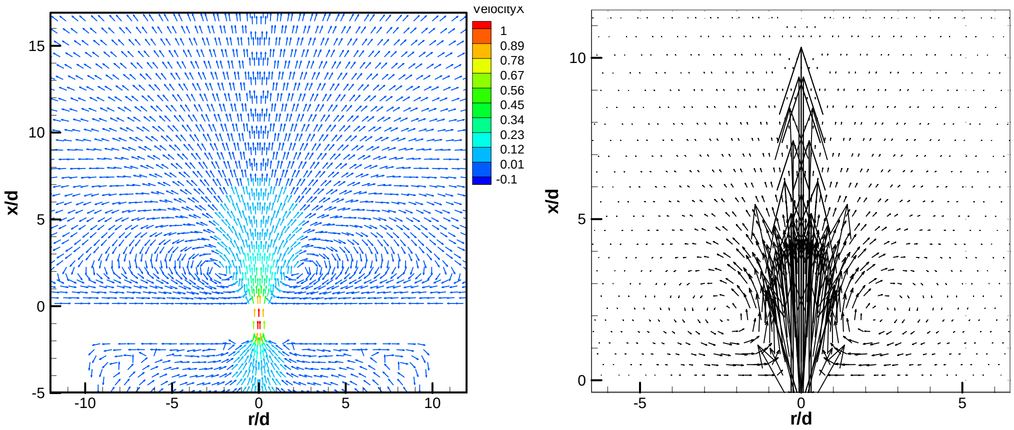

(b) t=4.2

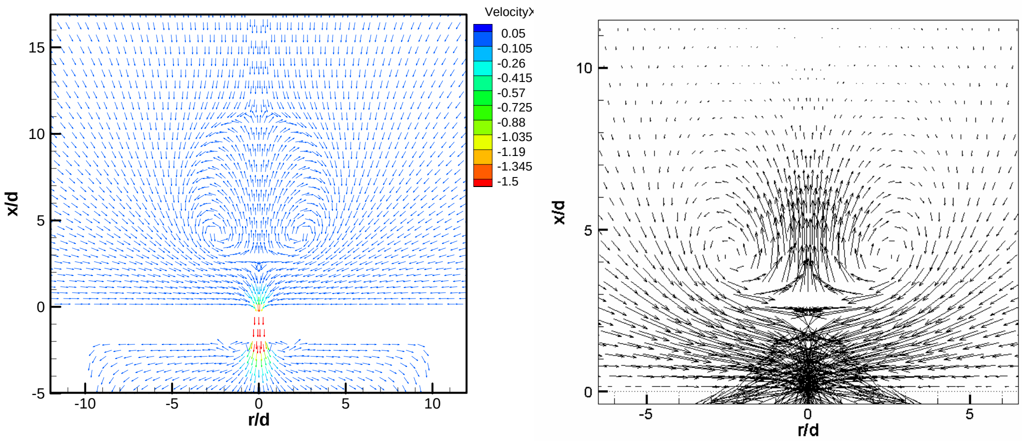

(c) t=4.4

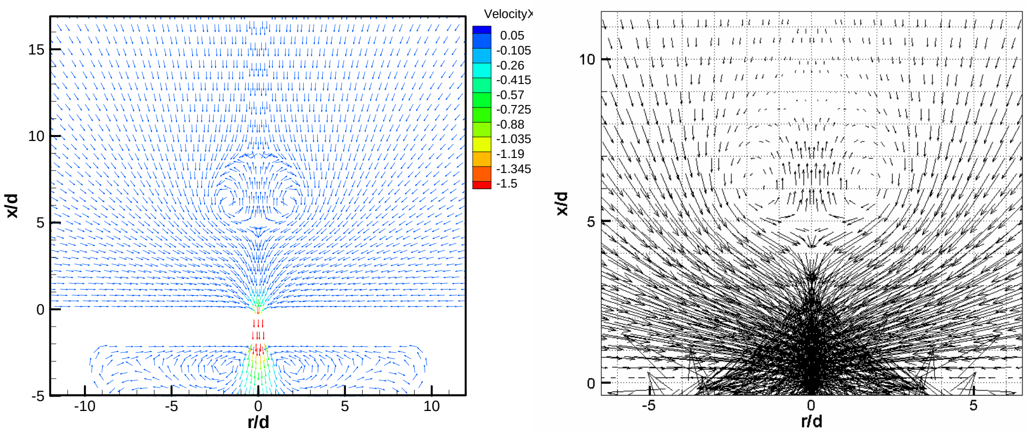

(d) t=4.6

Figure 2. Velocity fields at the different time instants of the cycle for Re=7.5.

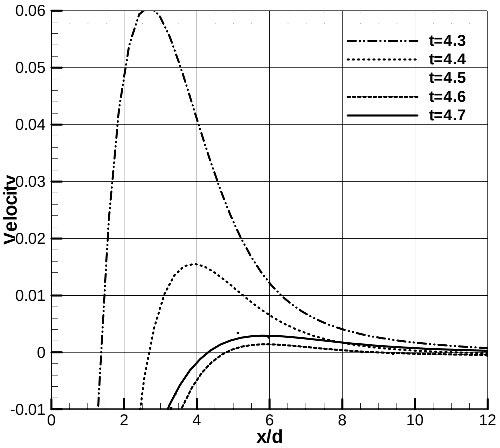

Figure 3. Distribution of axial velocity along the jet centre-line, *Re*=7.5.

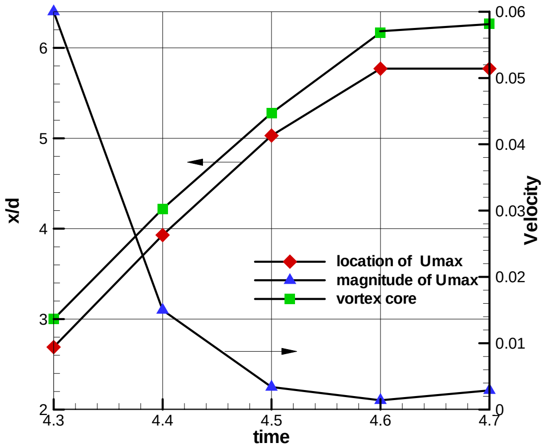

Figure 4. Movement of vortex core and of maximum centreline velocity, *Re*=7.5

The magnitudes and locations of the maximum velocity on the centreline as well as the vertical location of the centre of the vortex core during the suction period are shown in Figure 4. The maximum velocity gradually reduces from the beginning of the ingestion at t = 4.25 to a minimum between t = 4.6 and t = 4.7, and then increases. Although the increase in the maximum velocity is small it has occurred well before the end of the suction phase at t = 4.75, so that energy had to be supplied from somewhere. As the end of the suction phase is approached, the velocities towards the orifice are reduced. As a consequence, the rotational inertia of the vortex together with the remaining inertia of the jet provides the necessary energy to overcome the reducing velocity towards the orifice. The toroidal vortex, is able not only to sustain the jet, but in fact accelerates it! It is therefore interesting, as may be seen in Figure 4, to note that the motion of the core and the position of the maximum velocity move in concert with the vortex being slightly ahead of the vertical location of the maximum velocity. Towards the end of ingestion the vortex has lost much of its energy so that it has stopped moving away from the wall, as has the location of the maximum velocity. Thus it is clear that at least towards the end of ingestion, the vortex has sustained the jet.

As may be seen in Figure 5, the well-established synthetic jet, such as one with Re=23.5, behaves differently to the near limiting case with Re=7.5. Similarly to Figure 2, on the left side of Figure 5, the velocity fields at different times in the fourth cycle are visualised by vectors of constant length coloured by the non-dimensional axial velocity, whereas on the right side of Figure 5, the area near the orifice has been enlarged with the flow field still visualised with vectors of constant length, but with contours of constant vorticity $\tilde{\zeta}$, ($\tilde{\zeta} = \nabla \times \tilde{V}$) superimposed on the velocity fields. At the time of maximum expulsion (Figure 5a), both, two vortices can be seen; one near the orifice is a newly generated vortex, called an emerging vortex, whilst further away there is a lingering vortex, which is the remnant of merged vortices from previous cycles. The emerging vortex has been formed much further from the orifice that was the case in at Re = 7.2 as may be seen by comparing Figures 5(a and b) and 2(a).

By t=4.2 the emerging vortex has combined with the lingering vortex, but at this stage the two have not completely merged as may be seen by the highly distorted flow field in

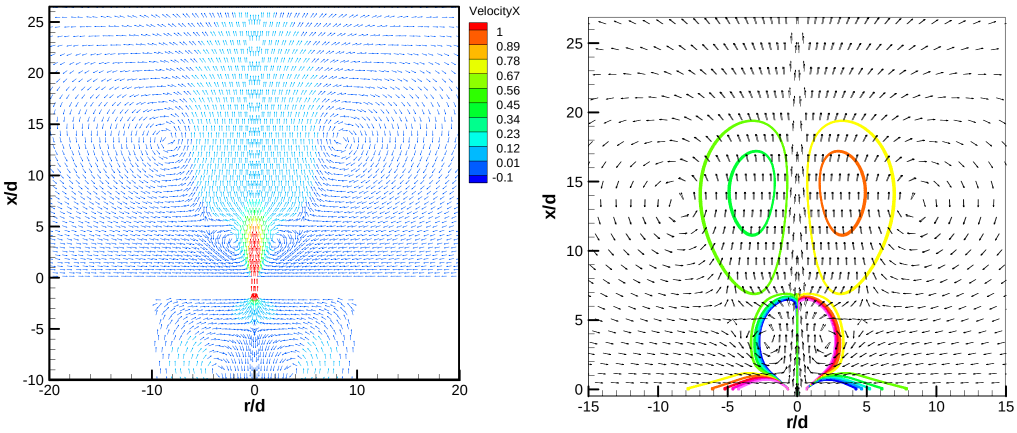

(a) t=4.0

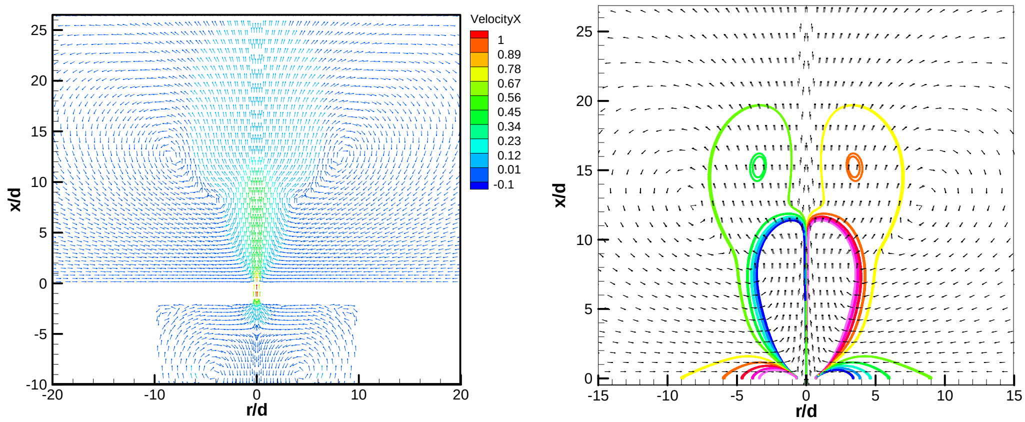

(b) *t*=4.2

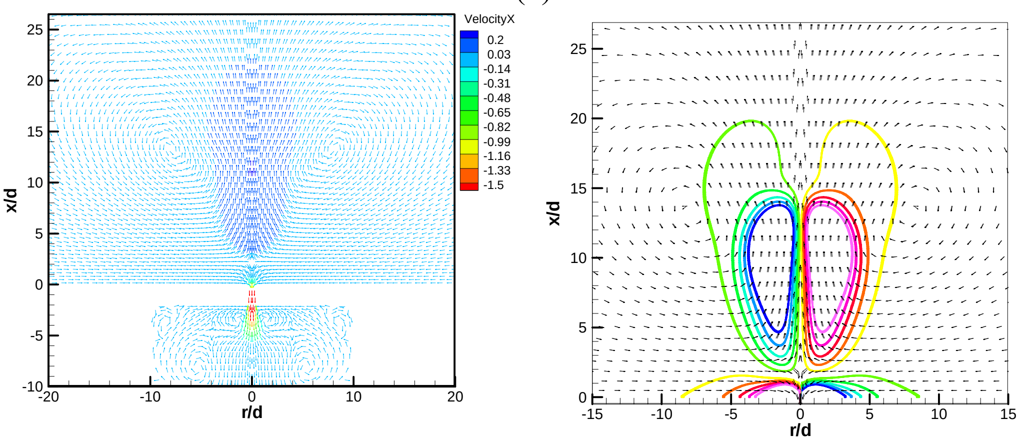

(c) *t*=4.4

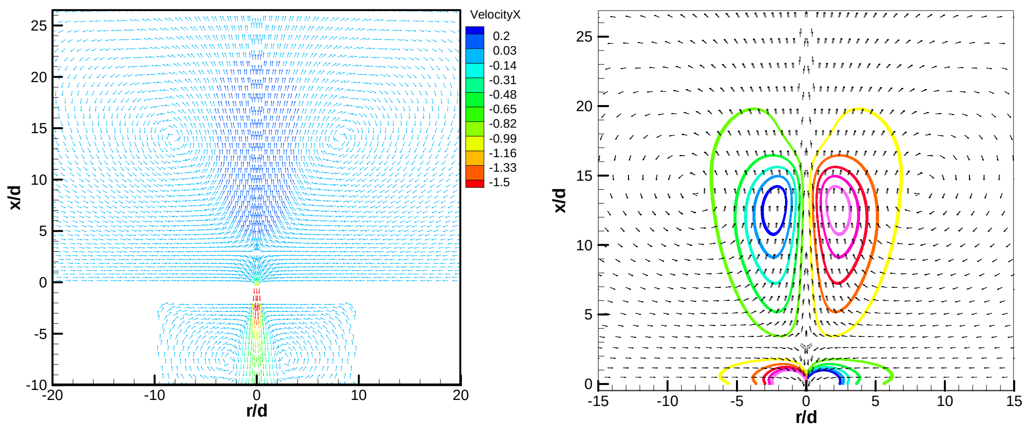

(d) t=4.6

Figure 5. Velocity fields at the different time instants of the cycle for Re=23.5.

the region defined by $3 < r/d < 10$ and $6 < x/d < 14$. However, at t=4.4 the emerging vortex, has now completely merged with the lingering vortex. It is clear from Figures 5 and 7 that the lingering vortex does not move far. Although not shown here, unfortunately the position of the core is slightly higher at t = 5.0 than at t = 4.0, so that the "approximately periodic" condition mentioned above was not satisfied in this case.

Whereas the remnant of the vortex, when Re = 7.5, was wiped out, certainly by the time of maximum expulsion, (Figure (2a)), and therefore there was no merging of vortices, when there is a lingering vortex the emerging vortex reinforces the existing vortex as was originally proposed by Mallinson *et al.* [9]. They interpreted the location of the maximum vorticity as being the location of the core.

At the time of maximum expulsion the strong vorticity region near the orifice encompasses the emerging vortex as may be seen in the right hand side of Figure 5(a).

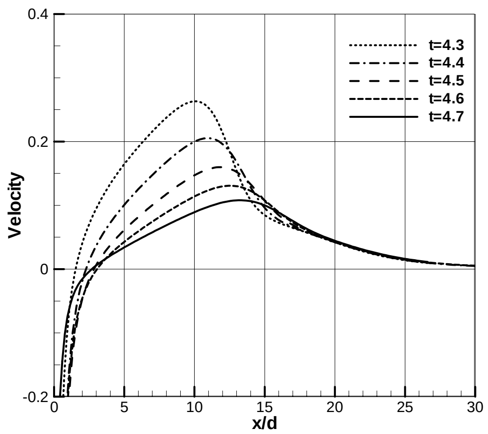

Figure 6. Distribution of axial velocity along the jet centre-line, Re=23.5.

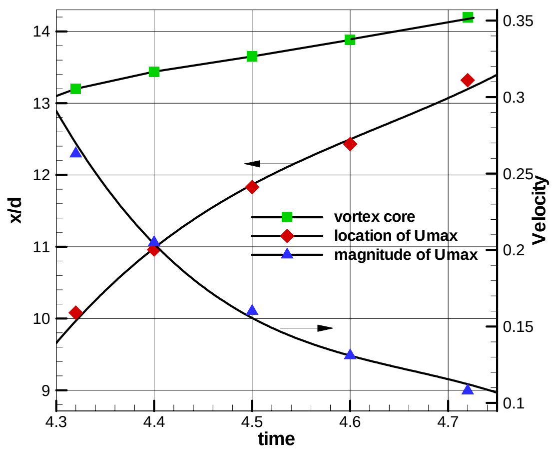

Figure 7. Movement of vortex core and maximum centreline velocity, Re=23.5.

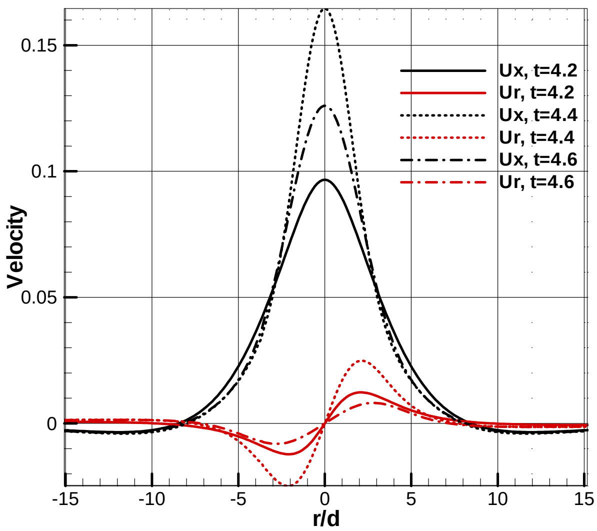

Figure 8. Axial and radial velocity at the plane of vortex core for Re=23.5.

However, the region of high vorticity further down stream clearly does not enclose the lingering vortex. This is even more apparent in Figure 5(b, c and d) in which the core of the toroidal vortex is clearly outside the region of high vorticity. The regions of high vorticity has a similar behaviour to the lingering and emerging vortices discussed in the previous paragraphs, but cannot be used as a possible explanation of the method of sustaining a jet as was done by Mallinson *et al* [9].

The distribution of the axial velocity along the centre-line for the suction stage for *Re* = 23.5 is shown in Figure 6. At this Reynolds number, downstream of the maximum velocity, the jet develops in a manner similar to a steady jet as had already been detected for much larger, apparently turbulent jets [6]. Here, the lingering vortex is located further away from the orifice, so that the maximum velocity reduces throughout the ingestion period and the minimum velocity is reached only at the end of that period. This is clearly illustrated in Figure 7 in which the magnitude and location of maximum centreline velocity during the ingestion period are presented together with location of lingering vortex core. Again towards the end of the intake period the vortices sustain the jet, as is clearly indicated in Figure 7 by the fact that the vertical location of the maximum velocity approaches the vertical location of the vortex centre.

Figure 8 shows profiles of axial and radial velocity at different times for *Re*=23.5 extracted at the horizontal planes passing through the vortex core. The maximum axial velocity is reached at t = 4.4 well after the point of maximum expulsion at the orifice (t = 4.0) and well after the ingestion phase has begun (t = 4.25). Time is needed to travel from the orifice starting when the ejection at its maximum, to reach the plane located at approximately x/d =13 is about 0.4 of a cycle. This simply explains how the maximum velocity occurs so late at a location far from the orifice. It follows that the interpretation of data concerning synthetic jets needs to be performed with great care; otherwise erroneous conclusions may be reached.

4. Conclusion

The evolution of micro synthetic jets in the ambient flow has been studied using numerical flow visualization. Vortex pair trajectories were visualized by extracting the vortex cores from the flow data. Results show that propagation of the vortices strongly depends on Reynolds number and the behaviour of well established jet (Re=23.5) is different from the limiting case (Re=7.5) when a jet has just been formed. In the case of *Re*=23.5 the lingering vortex even being week is clearly still present in the beginning of next expulsion stage. It was demonstrated that centreline jet velocity reveals the propagation of vortex rings and dynamics of its peak value corresponds to the movement of the vortex cores. Furthermore, it was shown that the location of maximum vorticity could not be used to identify the location of the core.

5. References

1. A. Glezer and M. Amitay, Synthetic jets, *Ann. Rev. Fluid Mech.*, **34**, pp503-529, 2002.
2. S.Yuan, Z. Zhou, Wang, C. Liu, MEMS-based piezoelectric array microjet, *Microelectronic engineering*, 66, pp.767-772, 2003.
3. D.S.Kercher, J-B. Lee, O. Brand, M. Allen, A. Glezer, "Microjet Cooling Devices for Thermal Management of Electronics." IEEE Transactions on Components & Packaging Technologies, 26(2):pp. 359-366, 2003.

4. Y. Utturkar, R. Holman, R. Mittal, B. Carrol, M. Sheplak and L. Cattafesta, A jet formation criterion for synthetic jet actuators, 41st Aerospace Sciences Meeting and Exhibit, 6-9 January Reno NV, AIAA 2003-0636, 2003.
5. V. Timchenko, J. Reizes, E. Leonardi and G. de Vahl Davis, 'A Criterion for the Formation of Micro Synthetic Jets', *2004 IMECE,* Anaheim, CA USA, November 13-19, 2004.
6. S.G. Mallinson, C.Y. Kwok and J.A. Reizes, Numerical simulation of micro-fabricated zero mass-flux jet actuators, *Sensors and Actuators* A 105 229-236, 2003.
7. G. Karniadakis, A. Beskok, *Micro flows: fundamentals and simulation*, Springer-Verlag New York Inc., 2002.
8. V. Timchenko, J.A. Reizes and E. Leonardi, 'Compressibility effects in micro synthetic jets', *2nd Int. Conference on Microchannels and Minichannels [ICMM2004]*, S.G. Kandlikar (ed), ASME, New York, pp. 273-280, 2004.
9. S.G. Mallinson, G. Hong, J.A. Reizes, Some Characteristics of Synthetic Jets, AIAA-99-3651, 30th AIAA Fluid Dynamics Conference, Nerfolk, VA, 1999.
10. M. Roth, Automatic Extraction of Vortex Core Lines and Other Line-Type Features for Scientific Visualization, Ph.D., ETH Zürich Institute of Scientific Computing Computer Graphics Group, 2000.